blood®
Brief Report

IMMUNOBIOLOGY AND IMMUNOTHERAPY

Copper 64–labeled daratumumab as a PET/CT imaging tracer for multiple myeloma

Enrico Caserta,[1,2,*] Junie Chea,[3,*] Megan Minnix,[3] Erasmus K. Poku,[3] Domenico Viola,[1,2] Steven Vonderfecht,[4] Paul Yazaki,[3] Desiree Crow,[3] Jihane Khalife,[1,2] James F. Sanchez,[2] Joycelynne M. Palmer,[5] Susanta Hui,[6] Nadia Carlesso,[1] Jonathan Keats,[7] Young Kim,[8] Ralf Buettner,[2] Guido Marcucci,[1] Steven Rosen,[2] John Shively,[3] David Colcher,[3] Amrita Krishnan,[2] and Flavia Pichiorri[1,2]

[1]Department of Hematologic Malignancies Translational Science, Beckman Research Institute, City of Hope, Duarte, CA; [2]Briskin Myeloma Center, Department of Hematology and Hematopoietic Cell Transplantation, City of Hope, Duarte, CA; [3]Department of Molecular Immunology and [4]Center for Comparative Medicine, Beckman Research Institute, City of Hope, Duarte, CA; [5]Department of Information Sciences, Division of Biostatistics, City of Hope, Duarte, CA; [6]Department of Radiation Oncology, Beckman Research Institute, City of Hope, Duarte, CA; [7]Translational Genomics Research Institute, Phoenix, AZ; and [8]Department of Pathology, City of Hope, Duarte, CA

KEY POINTS

- Daratumumab conjugated with ^{64}Cu efficiently binds to CD38 on myeloma cells and was mainly detected in the bones of mice.
- PET/CT based on ^{64}Cu-radiolabeled daratumumab displays a higher resolution and specificity for detecting myeloma than does ^{18}F-FDG PET/CT.

As a growing number of patients with multiple myeloma (MM) respond to upfront therapies while eventually relapsing in a time frame that is often unpredictable, attention has increasingly focused on developing novel diagnostic criteria to also account for disease dissemination. Positron emission tomography/computed tomography (PET/CT) is often used as a noninvasive monitoring strategy to assess cancer cell dissemination, but because the uptake of the currently used radiotracer 18fluorodeoxyglucose (^{18}F-FDG) is a function of the metabolic activity of both malignant and nonmalignant cells, the results frequently lack sufficient specificity. Radiolabeled antibodies targeting MM tissue may detect disease irrespective of cell metabolism. Hence, we conjugated the clinically significant CD38-directed human antibody daratumumab (Darzalex [Dara]) to the DOTA chelator and labeled it with the positron-emitting radionuclide copper 64 (^{64}Cu; ^{64}Cu-DOTA-Dara). Here, we show that ^{64}Cu-DOTA-Dara can efficiently bind CD38 on the surface of MM cells and was mainly detected in the bones associated with tumor in a MM murine model. We also show that PET/CT based on ^{64}Cu-DOTA-Dara displays a higher resolution and specificity to detect MM cell dissemination than does ^{18}F-FDG PET/CT and was even more sensitive than were bioluminescence signals. We therefore have supporting evidence for using ^{64}Cu-DOTA-Dara as a novel imaging agent for MM. (*Blood*. 2018;131(7):741-745)

Introduction

Prognostic information to stratify multiple myeloma (MM) patients into distinct risk-based treatments is currently based on specific genetic and cytogenetic abnormalities and clinical characteristics.[1,2] However, the extensive heterogeneity in therapeutic response, even in patients sharing similar characteristics,[1,2] emphasizes the need for more accurate prognostic tools.

Positron emission tomography/computed tomography using fluorodeoxyglucose-18 (^{18}F-FDG PET/CT) imaging in newly diagnosed MM patients correlates with progression-free survival.[3,4] 18F-FDG PET/CT also predicts the progression rate from smoldering MM to active disease.[5] Hence, most investigators now agree on the importance of using imaging as a prognostic criterion for MM.[6-8]

However, despite widespread use of ^{18}F-FDG PET/CT, its ability to detect malignancies is dependent on metabolic activity. Lesions with a low metabolic rate may therefore be undetectable. In fact, low expression of hexokinase-2 in MM cells is associated with false-negative ^{18}F-FDG PET/CT in MM.[9] By binding to a tumor antigen rather than relying on the metabolic state of a malignancy, antibody-based approaches may allow imaging of cancer cells with low metabolic activity. In support, the chimeric fibril-reactive monoclonal antibody can be used in patients with light chain–associated amyloidosis to identify candidates for passive immunotherapy.[10,11]

Daratumumab (Dara), a human anti-CD38 immunoglobulin G_1 (κ subclass) antibody against the highly expressed plasma cell receptor CD38, has shown particularly efficacious clinical activity[12-16] and recently has been approved by the US Food and Drug Administration for the treatment of relapsed MM. Because almost all MM patients express CD38 on the surface of their cancer cells, we hypothesize that tracing MM cell dissemination by targeting CD38 could be a successful approach.

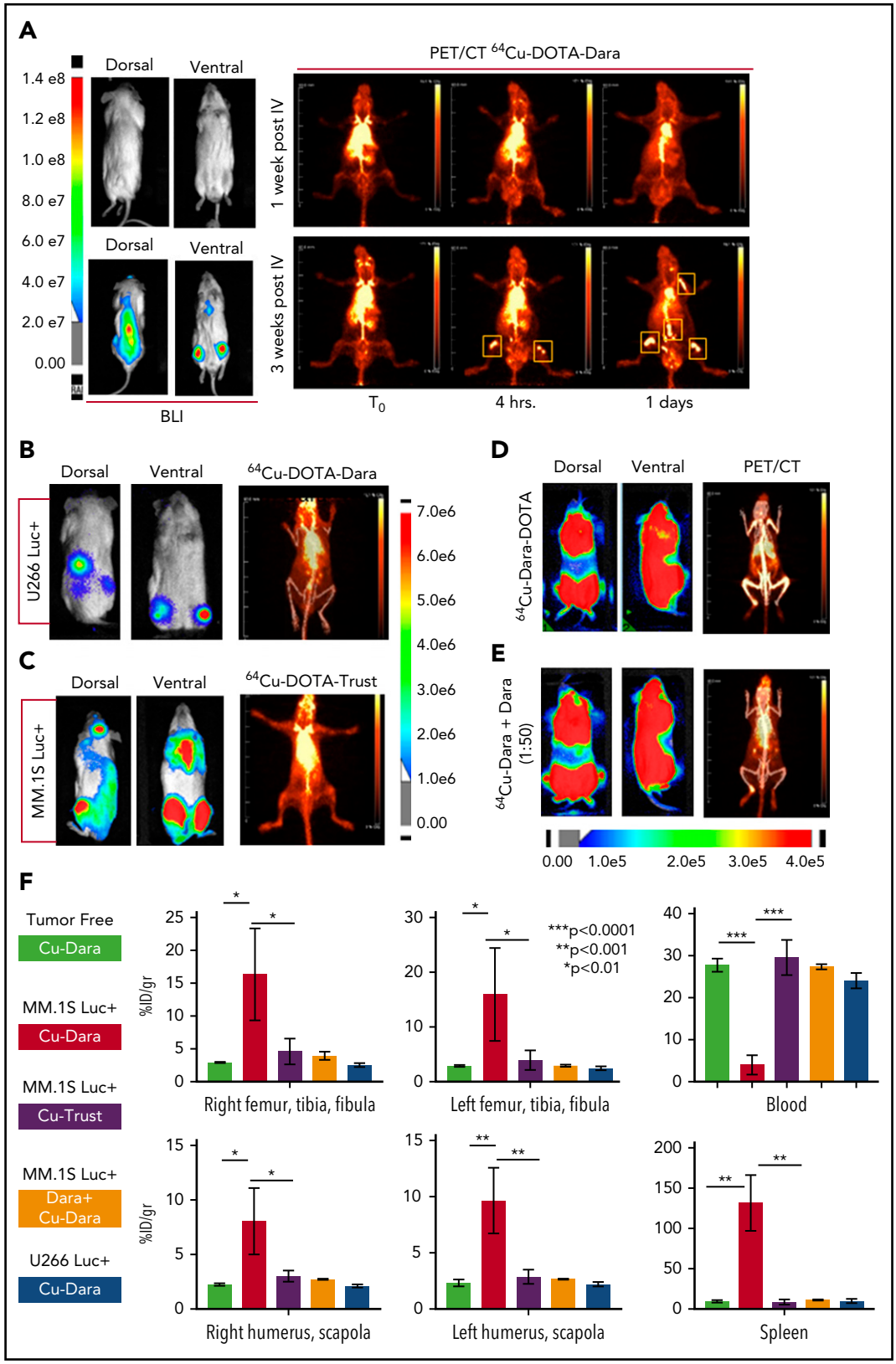

Figure 1. ^{64}Cu-DOTA-Dara detects MM cell dissemination in vivo. (A) The radiolabeled antibody ^{64}Cu-DOTA-Dara (3.7 MBq, 10 μg) was administered to 3 mice that had been transplanted by IV injection with a human MM cell line (MM.1S GFP$^+$/Luc$^+$) before (7 days post-IV) and after (21 days post-IV) signs of MM bone metastasis as detected by BLI. The mice were also imaged with ^{64}Cu-DOTA-Dara radiolabeled antibody on the following days, and PET imaging identified MM cell dissemination in the bone (yellow boxes), which overlap with the BLI signals in the same mouse. (B) ^{64}Cu-DOTA-Dara (3.7 MBq, 10 μg) was also administered to 2 mice that had been transplanted by IV injection with U266 Luc$^+$ MM cells, when clear signs (5 weeks post-IV) of MM bone engraftment were detected by BLI. The mice were imaged with ^{64}Cu-DOTA-Dara radiolabeled antibody after 1 day from the radiolabeled Dara injection (see also supplemental Figure 4B). Of note, no sign of engraftment was observed by PET/CT scan. (C) ^{64}Cu-DOTA-trastuzumab (^{64}Cu-DOTA-trast)

Study design

See the supplemental Methods section, available on the *Blood* Web site.

Results and discussion

The conjugation of Dara to DOTA was successful, as was demonstrated by gel electrophoresis (supplemental Figure 1A-B); DOTA-Dara was labeled with copper 64 (^{64}Cu) efficiently, with no evidence of aggregates (supplemental Figure 1C-D). The immunoreactivity of ^{64}Cu-DOTA-Dara preparations was >95% (supplemental Figure 1E). ^{64}Cu-DOTA-Dara was extremely stable up to 48 hours in saline solution and in mouse serum (supplemental Figure 2A-B). CD38-positive MM.1S green fluorescent protein/luciferase-positive (GFP$^+$/Luc$^+$) and CD38-negative U266 Luc$^+$ MM cells,[17] which express CD38 antigen at the same levels as do the respective parental cell lines (supplemental Figure 3A-B), were used to assess ^{64}Cu-DOTA-Dara specificity in vivo. Mice were analyzed 7 and 21 days after MM.1S GFP$^+$/Luc$^+$ cell injection. Each animal was then injected with the radiolabeled antibody 24 hours after bioluminescence (BLI) assessment and imaged immediately (T_0), at 4 hours and at days 1 and 2 after the injection (Figure 1A; supplemental Figure 4A). Both BLI and ^{64}Cu-DOTA-Dara PET/CT imaging of the same mice suggested absence of MM bone engraftment in the mice imaged at day 7, but both methods detected signals at day 21 (Figure 1A). No positive bone signs were indicated in nonengrafted mice or in mice engrafted with U266 Luc$^+$ cells (Figure 1B; supplemental Figure 4B). Lack of bone signaling was also observed in mice engrafted with MM.1S GFP$^+$/Luc$^+$ cells but imaged by a MM nonspecific radiolabeled antibody (^{64}Cu-trastuzumab-DOTA [^{64}Cu-trast-DOTA]) (Figure 1C), and when unlabeled Dara (cold) (50:1 excess) was used in combination with ^{64}Cu-DOTA-Dara (Figure 1D-E; supplemental Figure 4C). Ex vivo biodistribution studies at 24 hours verified the trends observed through PET analysis (Figure 1F). ^{64}Cu-DOTA-Dara was significantly detectable in MM.1S-engrafted mice (n = 4) in comparison with the tumor-free mice (n = 4) and with the mice injected with ^{64}Cu-trast-DOTA (n = 3) in the femurs, tibias, humeri, and scapola, known sites of MM cell invasion (Figure 1F). The same biodistribution trend observed in the control mice was observed in the organs of the mice injected with U266 cells or with cold unlabeled Dara (1:50) (Figure 1F). Higher signals were also observed in all organs made of bone tissue such as sternum, skull, and spinal column and in the lung (supplemental Figure 5A-B). ^{64}Cu-DOTA-Dara was also significantly detected in the spleen of MM.1S GFP$^+$/Luc$^+$–engrafted mice (Figure 1F; supplemental Figure 5A), which was also confirmed by flow cytometry (supplemental Figure 5B). In contrast, the majority of ^{64}Cu-DOTA-Dara remained in the blood of the control mice ($P < .0001$) and was not significantly different in the other organs (supplemental Figure 5A). To assess the sensitivity of the ^{64}Cu-Dara signal in comparison with the standard ^{18}F-FDG PET-CT scan, we analyzed an independent group of animals bearing CD38$^+$ tumors. At 21 days after cell injection, mice were first assessed by BLI and then injected with ^{18}F-FDG (Figure 2A-B). The same group of mice were then injected with ^{64}Cu-DOTA-Dara the next day, and PET imaging was performed (Figure 2C; supplemental video A). BLI and ^{64}Cu-DOTA-Dara PET/CT revealed the presence of MM cells, whereas tumors were almost undetectable with the ^{18}F-FDG PET/CT (Figure 2C-D). The ^{18}F-FDG PET signals were mainly associated with the nonspecific uptake of glucose in leg muscles and the brain. The ^{18}F-FDG bone signal was almost equal to the background signal of ^{18}F-FDG in the heart, a contrast to the highly specific bone signal detected by ^{64}Cu-DOTA-Dara (Figure 2D; see also supplemental videos A and B).

To assess the ability of ^{64}Cu-DOTA-Dara to recognize MM cells in the bones when the BLI signal was minimal or completely absent, we used an independent group of mice for histology analysis and for immunohistochemical staining for the MM cell marker CD138. Step section of the bones show foci of MM cells, as is also assessed by CD138 staining in the right and left femurs, confirming the presence of MM cells in the location where both BLI and ^{64}Cu-DOTA-Dara signals were present (Figure 2E-G). We also detected MM cells in the lower vertebral body, which had no BLI signal (Figure 2E-G) and no cells in the humerus, which was also found negative by PET/CT scan (Figure 2E-G).

The relatively short half-life of ^{64}Cu (12.7 hours) may be ideal for patient safety and is sufficiently long for PET/CT imaging up to 48 hours after administration. We have used ^{64}Cu-labeled trastuzumab to safely detect human epidermal growth factor receptor 2 (HER2)–positive tissue in metastatic breast cancer (MBC) patients.[18] ^{64}Cu was safe, and by day 1 after injection, ^{64}Cu-trastuzumab-DOTA was able to detect MBC, its binding correlating with patient HER2 status. Although Dara has been conjugated with the radionuclide ^{89}zirconium (^{89}Zr),[19] the tendency of ^{89}Zr to accumulate in the bones,[19-21] associated with a longer time requested for imaging in contrast to ^{64}Cu, may be a limitation in specifically detecting MM cell dissemination in the bones. Our data clearly show higher sensitivity of ^{64}Cu-Dara-DOTA not only in comparison with ^{18}F-FDG signal but also in comparison with BLI imaging, an effect that was not seen when Dara was conjugated with ^{89}Zr.[19] Because our studies show a high sensitivity of ^{64}Cu-Dara-DOTA in detecting MM cells, we believe that this imaging approach for MM may also be clinically relevant for detecting minimal residual disease (MRD). MRD, as detected by high throughput bone marrow DNA sequencing, is being considered as a surrogate endpoint in clinical trials,[22-24] because effective therapies necessitate 5 to 10 years of follow-up to detect differences in survival.[25,26] However, irrespective of its sensitivity, this technique is marrow based and cannot

Figure 1 (continued) (3.7 MBq, 10 μg) was administrated to 3 MM.1S GFP$^+$/Luc$^+$–engrafted mice, as assessed by BLI imaging, and a PET/CT scan was performed 1 day after ^{64}Cu-DOTA-trast injection. No bone signals were observed, but only high background associated with the circulating radiolabeled antibody. (D-E) Mice bearing CD38$^+$ MM cells (MM.1S GFP$^+$/Luc$^+$) with a high level of engraftment (see also supplemental Figure 4C), as assessed by BLI images, that were injected with ^{64}Cu-DOTA-Dara (3.7 MBq, 10 μg) without (D) and with (E) unlabeled Dara (500 μg) and imaged at day 1 by PET/CT. Almost no signs of engraftments were detected in the presence of cold Dara, independent of the BLI signals. (F) ^{64}Cu-DOTA-Dara PET/CT-positive mice (MM.1S GFP$^+$/Luc$^+$–engrafted mice: 4) and negative mice (tumor free mice: 4); ^{64}Cu-DOTA-trast–treated mice (3); unlabeled Dara (Block) treated mice (2); and U266-engrafted mice (2) were sacrificed, and organs were harvested at 24 hours and used for γ counting to determine their radioactive content, as is presented in the bar graphs as a percentage of the injected dose per gram (%ID/g). See also supplemental Figure 5A.

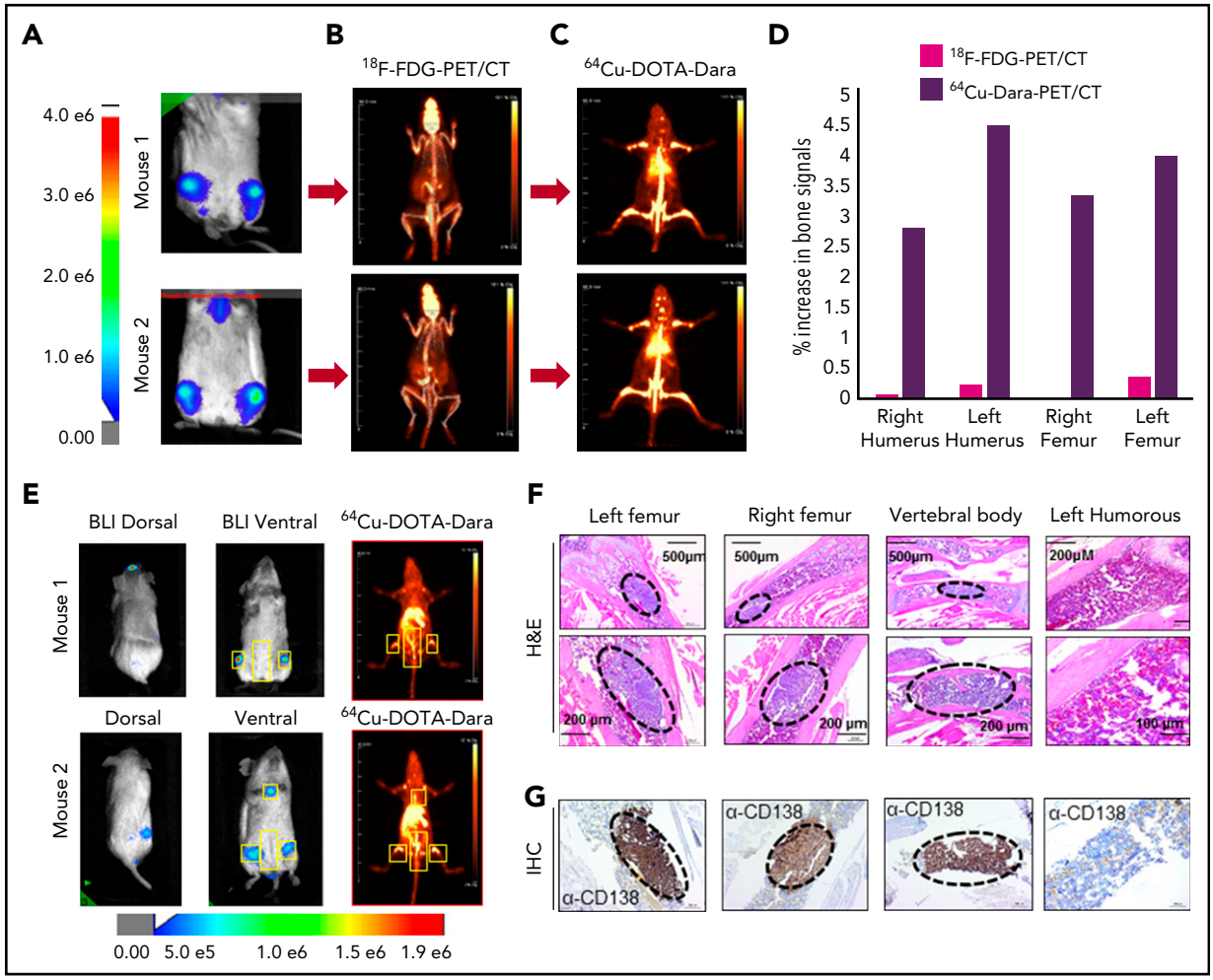

Figure 2. ^{64}Cu-DOTA-Dara PET/CT shows higher resolution than does ^{18}F-FDG-PET/CT. (A-C) Representative images of 2 NSG mice (mouse 1 and mouse 2), which were injected with 5 × 10^6 MM.1S GFP$^+$/Luc$^+$ cells. After 2 weeks from the injection, the mice were imaged using BLI (A), and after 24 hours, the same mice were imaged by ^{18}F-FDG-PET (B). The day after, ^{64}Cu-DOTA-Dara (3.7 MBq, 10 µg) was administered to the same mice imaged with ^{18}F-FDG-PET and BLI (C). (D) Graphical representation of the intensity of the signal of ^{64}Cu-DOTA-Dara PET/CT in comparison with ^{18}F-FDG-PET/CT, expressed as a percentage of the increase in percentage of the injected dose per gram (%ID/gr) of bone organs in comparison with the nonspecific signal of each radio nucleotide (%ID/gr) detected in the heart. A radiolabeled antibody identified MM cancer cells, which were undetectable by ^{18}F-FDG-PET scan. (E) Mice with minimum BLI signals were IV-injected with ^{64}Cu-DOTA-Dara (3.7 MBq, 10 µg) and then imaged by PET/CT, which identified MM cell dissemination in the bone (yellow boxes). (F-G) Representative images at different magnifications of tissue sections stained by hematoxylin and eosin stain (F) and CD138 immunohistochemical stain (G) showing MM cell accumulation (black dashed ovals) in the left and right femurs and in the vertebral body (lower lumbar), but not in the left humerus, which did not show PET/CT signals. H&E, hematoxylin and eosin; IHC, immunohistochemical.

account for a nonhomogenous bone marrow infiltration and extramedullary involvement. In support of Dara as a unique tool for imaging in MM, our group developed a ^{64}Cu antibody (elotuzumab [Elo]) against the highly specific MM receptor CS1 (^{64}Cu-DOTA-Elo). Although ^{64}Cu-DOTA-Elo bound the CS1 antigen in vitro, it did not identify bone engraftment of CS1-positive MM cells in in vivo studies (data not shown). We have begun a ^{64}Cu-DOTA-Dara PET/CT imaging trial that has the potential to affect MM clinical cell detection.

Acknowledgments

The authors acknowledge Dori Triplett, Evelyn Flores, and Debbie Flood for administrative support. Research reported in this publication included work performed in the Center for Biomedicine and Genetics facility.

This work was supported by a Steven Gordon and Briskin Family Innovation Grant (F.P., D.C., J.S.). The Small Animal Imaging Center City of Hope (COH) core and Pathology core used for immunohistochemical staining were supported by the National Institutes of Health National Cancer Institute (P30CA033572) and by the COH Veterinary Pathology Program. The content is solely the responsibility of the authors and does not necessarily represent the official views of the National Institutes of Health.

Authorship

Contribution: E.C., S.H., J.K., S.R., J.S., N.C., D.C., A.K., and F.P. designed the research; E.C., J.C., M.M., E.K.P., D.V., S.V., J.K., P.Y., Y.K., and R.B. performed the research; E.C., J.F.S., J.M.P., G.M., J.S., D.C., and F.P. analyzed the data; J.F.S. and F.P. wrote the manuscript; and all authors reviewed the manuscript.

Conflict-of-interest disclosure: A.K. is a consultant for and on the speakers' bureau of Janssen Pharmaceuticals. The remaining authors declare no competing financial interests.

Correspondence: Flavia Pichiorri, Department of Hematology and Hematopoietic Cell Transplantation, City of Hope, 1500 E Duarte Rd, Duarte, CA 91010; e-mail: fpichiorri@coh.org; and David Colcher,

Department of Molecular Immunology, City of Hope, 1500 E Duarte Rd, Duarte, CA 91010; e-mail: dcolcher@coh.org.

*E.C. and J.C. contributed equally to this work.

The online version of this article contains a data supplement.

The publication costs of this article were defrayed in part by page charge payment. Therefore, and solely to indicate this fact, this article is hereby marked "advertisement" in accordance with 18 USC section 1734.

Footnotes

Submitted 19 September 2017; accepted 27 December 2017. Prepublished online as *Blood* First Edition paper, 4 January 2018; DOI 10.1182/blood-2017-09-807263.

REFERENCES

1. Richardson P, Mitsiades C, Schlossman R, et al. The treatment of relapsed and refractory multiple myeloma. *Hematology Am Soc Hematol Educ Program*. 2007;2007:317-323.
2. Anderson KC, Kyle RA, Rajkumar SV, Stewart AK, Weber D, Richardson P; ASH/FDA Panel on Clinical Endpoints in Multiple Myeloma. Clinically relevant end points and new drug approvals for myeloma. *Leukemia*. 2008;22(2):231-239.
3. Bartel TB, Haessler J, Brown TL, et al. F18-fluorodeoxyglucose positron emission tomography in the context of other imaging techniques and prognostic factors in multiple myeloma. *Blood*. 2009;114(10):2068-2076.
4. Zamagni E, Patriarca F, Nanni C, et al. Prognostic relevance of 18-F FDG PET/CT in newly diagnosed multiple myeloma patients treated with up-front autologous transplantation. *Blood*. 2011;118(23):5989-5995.
5. Zamagni E, Nanni C, Gay F, et al. 18F-FDG PET/CT focal, but not osteolytic, lesions predict the progression of smoldering myeloma to active disease. *Leukemia*. 2016;30(2):417-422.
6. Cavo M, Terpos E, Nanni C, et al. Role of 18F-FDG PET/CT in the diagnosis and management of multiple myeloma and other plasma cell disorders: a consensus statement by the International Myeloma Working Group. *Lancet Oncol*. 2017;18(4):e206-e217.
7. Raza S, Leng S, Lentzsch S. The critical role of imaging in the management of multiple myeloma. *Curr Hematol Malig Rep*. 2017;12(3):168-175.
8. Kumar S, Paiva B, Anderson KC, et al. International Myeloma Working Group consensus criteria for response and minimal residual disease assessment in multiple myeloma. *Lancet Oncol*. 2016;17(8):e328-e346.
9. Rasche L, Angtuaco E, McDonald JE, et al. Low expression of hexokinase-2 is associated with false-negative FDG-positron emission tomography in multiple myeloma. *Blood*. 2017;130(1):30-34.
10. Wall JS, Kennel SJ, Stuckey AC, et al. Radioimmunodetection of amyloid deposits in patients with AL amyloidosis. *Blood*. 2010;116(13):2241-2244.
11. Edwards CV, Gould J, Langer AL, et al. Interim analysis of the phase 1a/b study of chimeric fibril-reactive monoclonal antibody 11-1F4 in patients with AL amyloidosis. *Amyloid*. 2017;24(supp 1):58-59.
12. Dimopoulos MA, Oriol A, Nahi H, et al; POLLUX Investigators. Daratumumab, lenalidomide, and dexamethasone for multiple myeloma. *N Engl J Med*. 2016;375(14):1319-1331.
13. Plesner T, Arkenau HT, Gimsing P, et al. Phase 1/2 study of daratumumab, lenalidomide, and dexamethasone for relapsed multiple myeloma. *Blood*. 2016;128(14):1821-1828.
14. Palumbo A, Chanan-Khan A, Weisel K, et al; CASTOR Investigators. Daratumumab, bortezomib, and dexamethasone for multiple myeloma. *N Engl J Med*. 2016;375(8):754-766.
15. Rajan AM, Kumar S. New investigational drugs with single-agent activity in multiple myeloma. *Blood Cancer J*. 2016;6(7):e451.
16. Lokhorst HM, Plesner T, Laubach JP, et al. Targeting CD38 with daratumumab monotherapy in multiple myeloma. *N Engl J Med*. 2015;373(13):1207-1219.
17. Pei XY, Dai Y, Felthousen J, et al. Circumvention of Mcl-1-dependent drug resistance by simultaneous Chk1 and MEK1/2 inhibition in human multiple myeloma cells. *PLoS One*. 2014;9(3):e89064.
18. Mortimer JE, Bading JR, Colcher DM, et al. Functional imaging of human epidermal growth factor receptor 2-positive metastatic breast cancer using (64)Cu-DOTA-trastuzumab PET. *J Nucl Med*. 2014;55(1):23-29.
19. Ghai A, Maji D, Cho N, et al. Preclinical development of CD38-targeted [89Zr]Zr-DFO-daratumumab for imaging multiple myeloma [published online ahead of print 12 October 2017]. *J Nucl Med*. doi:10.2967/jnumed.117.196063.
20. Asiedu K, Munira F, Ton A, Adler S, Choyke P, Sato N. Hematopoietic stem cell homing to bone injuries observed with Zr-89 oxine positron emission tomographic imaging. *J Nucl Med*. 2017;58(suppl 1):183.
21. van de Watering FC, Rijpkema M, Perk L, Brinkmann U, Oyen WJ, Boerman OC. Zirconium-89 labeled antibodies: a new tool for molecular imaging in cancer patients. *Biomed Res Int*. 2014;2014:203601.
22. Munshi NC, Anderson KC. Minimal residual disease in multiple myeloma. *J Clin Oncol*. 2013;31(20):2523-2526.
23. Landgren O, Gormley N, Turley D, et al. Flow cytometry detection of minimal residual disease in multiple myeloma: Lessons learned at FDA-NCI roundtable symposium. *Am J Hematol*. 2014;89(12):1159-1160.
24. Martinez-Lopez J, Lahuerta JJ, Pepin F, et al. Prognostic value of deep sequencing method for minimal residual disease detection in multiple myeloma. *Blood*. 2014;123(20):3073-3079.
25. Morgan GJ, Davies FE, Gregory WM, et al; National Cancer Research Institute Haematological Oncology Clinical Studies Group. Cyclophosphamide, thalidomide, and dexamethasone as induction therapy for newly diagnosed multiple myeloma patients destined for autologous stem-cell transplantation: MRC Myeloma IX randomized trial results. *Haematologica*. 2012;97(3):442-450.
26. Rawstron AC, Gregory WM, de Tute RM, et al. Minimal residual disease in myeloma by flow cytometry: independent prediction of survival benefit per log reduction. *Blood*. 2015;125(12):1932-1935.